Available online at www.sciencedirect.com

ScienceDirect

Procedia Engineering 6 (2010) 274–282

Procedia Engineering

www.elsevier.com/locate/procedia

IUTAM Symposium on Computational Aero-Acoustics for Aircraft Noise Prediction

Direct Numerical Simulations of Airfoil Self-Noise

R.D. Sandberg[a], L.E. Jones[a]

[a]*School of Engineering Sciences, University of Southampton, Southampton SO17 1BJ*

Abstract

Direct numerical simulations (DNS) of airfoil self-noise were conducted. For the low Reynolds number airfoil flows accessible by DNS, the occurrence of laminar separation bubbles involving laminar-turbulent transition and turbulent reattachment leads to additional noise sources other than the traditionally studied trailing-edge noise. Cross-correlations of acoustic and hydrodynamic quantities in conjunction with ray-acoustic theory are used to identify the main source locations for a NACA-0006 airfoil. It is found that the contribution of trailing edge noise dominates at low frequencies while for the high frequencies the radiated noise is mainly due to flow events in the reattachment region on the suction side. DNS have also been conducted of NACA-0012 airfoils with serrated and straight flat-plate trailing-edge extensions using a purposely developed immersed boundary method. Noise reduction for higher frequencies is shown and the effect of the trailing edge serrations on the acoustic feedback loop observed in previous simulations and the subsequent effect on the laminar separation bubble is studied.

Keywords: airfoil noise, direct numerical simulations

1. Introduction

Airfoil self-noise, i.e. noise produced by the interaction of an airfoil's boundary layers and wake with itself, is an important noise source in many applications, ranging from wind turbines and helicopter rotors to fan blades and airframes. Brooks *et al.*[1] classified five mechanisms for airfoil self-noise, relating all but one to the interaction of disturbances with the airfoil trailing edge (TE). This is partly due to the fact that fluctuations which encounter a sharp edge of a solid body (such as a TE) are scattered, which leads to a considerable increase in the radiated sound power (M^5-scaling [2]) over fluctuations in free space (M^8-scaling [3]). For that reason, TE noise is typically one of the main noise sources, particularly at low Mach numbers, and hence the development of trailing-edge noise theories has been given much attention. An important example is Amiet's classical trailing edge noise theory [4] which predicts the farfield noise produced by the turbulent flow over an airfoil using only the airfoil surface pressure difference as input.

Recent studies have reported the presence of additional noise sources distinct from sources at the airfoil trailing edge. In two-dimensional numerical simulations, Tam and Ju [5] observed that vortices in the airfoil wake may themselves generate pressure waves, while Sandberg *et al.*[6] noticed additional noise sources on the suction surface associated with vortex shedding caused by a laminar separation bubble. In a subsequent three-dimensional numerical study of an airfoil at incidence exhibiting a separation bubble, Sandberg *et al.* [7] also observed the transition/reattachment region to act as a source of noise distinct from the airfoil

1877-7058
doi:10.1016/j.proeng.2010.09.029

trailing edge, possessing markedly different directivity. Since these noise generation mechanisms are different from that occurring at the trailing-edge, classical methods based on surface pressure difference (e.g. Amiet's theory [4]) cannot predict the overall airfoil self-noise accurately. Therefore, one of the objectives of the current study is to determine the nature and significance of noise sources distinct from the TE noise mechanism.

Although the presence of additional noise sources might be important for certain flow conditions or airfoil geometries, for most practical applications the TE noise mechanism will dominate. Thus any successful airfoil self-noise reduction measures will have to address the trailing-edge noise mechanism. Previous experimental and analytical studies have shown that TE modifications can reduce airfoil self-noise without compromising aerodynamic performance. The addition of brushes to airfoil trailing edges, for example, was found to reduce the intensity of trailing-edge noise [8]. The noise reduction in that case is likely due to increased compliancy of the brushes weakening the diffraction effect at the airfoil trailing edge and alleviating the surface pressure difference.

Alternatively, TE serrations have been considered. Howe [9] performed a numerical analysis of a flat plate with TE serrations possessing sawtooth-like profiles and predicted that the intensity of TE noise radiation could be reduced by such modifications, with the magnitude of the reduction depending on the length and spanwise spacing of the teeth, and the frequency of the radiation. It was determined that longer, narrower teeth should yield a greater intensity reduction. Oerlemans *et al.* [10] investigated experimentally the effect of adding such TE serrations to full size wind-turbine blades and found overall self-noise reductions of 2-3dB without adversely affecting aerodynamic performance. Nevertheless, the precise mechanism by which this noise reduction occurs is not yet fully understood. Understanding those mechanisms could lead to improvements in serration design, and possibly the development of alternative techniques based on similar physical principles. This study therefore also aims at numerically investigating the flow around airfoils with trailing edge modifications to identify the mechanism by which the noise reduction effect is achieved.

Direct numerical simulation (DNS) is the preferred tool for such fundamental studies due to the absence of modelling. Compressible DNS allow an accurate representation of hydrodynamic phenomena such as turbulence and transition to turbulence, and of the propagation of acoustic waves. Conducting direct noise simulations avoids interfacing between solution methods as required for hybrid approaches, and allows for the presence of acoustic feed-back loops [11]. The complex geometries associated with trailing edge modifications represent a considerable numerical challenge using high-order accuracy spatial schemes, however. For this reason a purposely developed immersed boundary (IB) representing the trailing edge modification is employed.

2. Governing Equations

The DNS code directly solves the unsteady, compressible Navier-Stokes equations, written in nondimensional form as

$$\rho_{,t} + (\rho u_k)_{,k} = 0 \,, \tag{1}$$

$$(\rho u_i)_{,t} + [\rho u_i u_k + p\delta_{ik} - \tau_{ik}]_{,k} = 0 \,, \tag{2}$$

$$(\rho E)_{,t} + [u_k(\rho E + p) + q_k - u_i\tau_{ik}]_{,k} = 0 \,, \tag{3}$$

where the total energy is defined as $E = T/\left[\gamma(\gamma-1)M^2\right] + 0.5u_iu_i$. The stress tensor and the heat-flux vector are computed as

$$\tau_{ik} = \mu\left(u_{i,k} + u_{k,i} - 2/3u_{j,j}\delta_{ik}\right)/Re \quad , \quad q_k = -\mu T_{,k}/[(\gamma-1)M^2 PrRe] \,, \tag{4}$$

respectively, where the Prandtl number is assumed to be constant at $Pr = 0.72$, and $\gamma = 1.4$. The molecular viscosity μ is computed using Sutherland's law [12], setting the ratio of the Sutherland constant over freestream temperature to 0.36867. To close the system of equations, the pressure is obtained from the non-dimensional equation of state $p = (\rho T)/(\gamma M^2)$. The primitive variables ρ, u_i, and T have been nondimensionalized by the freestream conditions and the airfoil chord is used as the reference length scale. Dimensionless parameters Re, Pr and M are defined using free-stream (reference) flow properties.

3. Numerical Method

The finite-difference code used for the current investigation is based on a code extensively used for compressible turbulence research, such as compressible turbulent plane channel flow [13], or turbulent flow over a flat-plate trailing-edge [14]. The underlying numerical algorithm consists of a five-point fourth-order accurate central difference scheme combined with a fourth-order accurate Carpenter boundary scheme [15] for the spatial discretization, and an explicit fourth-order accurate Runge-Kutta scheme for time-stepping. No artificial viscosity or filtering is used. Instead, stability is enhanced by appropriate treatment of the viscous terms in combination with entropy splitting of the inviscid flux terms [13]. More recently the code was extended so that it could be applied to a C-type grid with wake connection. At the freestream boundary, where the only disturbances likely to reach the boundary will be in the form of acoustic waves, an integral characteristic boundary condition is applied [16], in addition to a sponge layer comprising a dissipation term added to the governing equations. At the downstream exit boundary, which is subject to the passage of nonlinear amplitude fluid structures, a zonal characteristic boundary condition [17] is applied for increased effectiveness. At the airfoil surface an adiabatic, no slip condition is applied. This variant of the code has been recently used for direct numerical simulations of transitional flows on full airfoil configurations [11, 18].

For simulations of airfoils with serrated and non-serrated flat-plate trailing-edge extensions an immersed boundary method (IBM) as described in Jones and Sandberg [19] was used. The purposely developed immersed boundary condition is applied by directly modifying the computational stencil used for discretizing the governing equations in the vicinity of the immersed boundary. Thereby, a 'sharp' boundary interface can be realized, in contrast to other methods that use distributed forcing functions. The accuracy of the method may readily be altered by selection of the derivative scheme employed at the immersed boundary itself, and in the vicinity of the immersed boundary when solving the governing equations. The method was found able to reproduce both bluff body shedding and TS-wave amplitudes to a high degree of accuracy, especially when compared to similar methods [19].

The influence of domain size and grid resolution have been investigated thoroughly for the flow around a NACA-0012 airfoil at $Re = 5 \times 10^4$ and $\alpha = 5^\circ$ in Jones *et al.*[18], and the conclusions reached were used as guidelines for the current studies. The C-type domain of all cases presented in the current study had the dimensions of 5 chord-lengths from the trailing edge to the outflow boundary, 7.3 chord-lengths from the airfoil surface to the freestream surface, and a spanwise width of 0.2 chords. In the tangential direction, 2570 grid points were used, with 1066 and 1126 points clustered over the airfoil for the cases without and with trailing edge extensions, respectively. In the lateral direction, 692 grid points were used and the spanwise domain was discretized with 96 points.

4. Identification of additional noise sources

In order to identify the main noise sources, cross-correlations between pressure recorded in the free-stream and at the airfoil surface are computed [20]. The pressure at a fixed measurement location in the free-stream, denoted $p_f(t)$, and the pressure recorded at the airfoil surface as a function of x, denoted $p_s(x,t)$ are considered. Cross correlations between the two variables are computed as a function of x and retarded time Δt as

$$C_{pp}(x,\Delta t) = \frac{S_{p_f(t+\Delta t)p_s(x,t)}}{\sigma_{p_f(t+\Delta t)}\sigma_{p_s(x,t)}}, \tag{5}$$

where S is the covariance and σ the standard deviation. In order to interpret the results correctly, the time taken for an acoustic wave originating at the airfoil surface to propagate to the free-stream measurement location must be known as a function of x. This is determined by a simple acoustic ray method, whereby ray vectors are integrated as a function of local velocity and sound-speed, coupled with a secant shooting algorithm. For the purposes of this study refraction effects are neglected, noting that variations in mean sound speed are less than 3% for the current case. Since the hydrodynamic and acoustic behaviour vary significantly with frequency, it is of interest to compute cross-correlations for finite frequency intervals. This is achieved by computing the Fourier transform of p_{free} and p_{surf}, setting the amplitude of modes outside

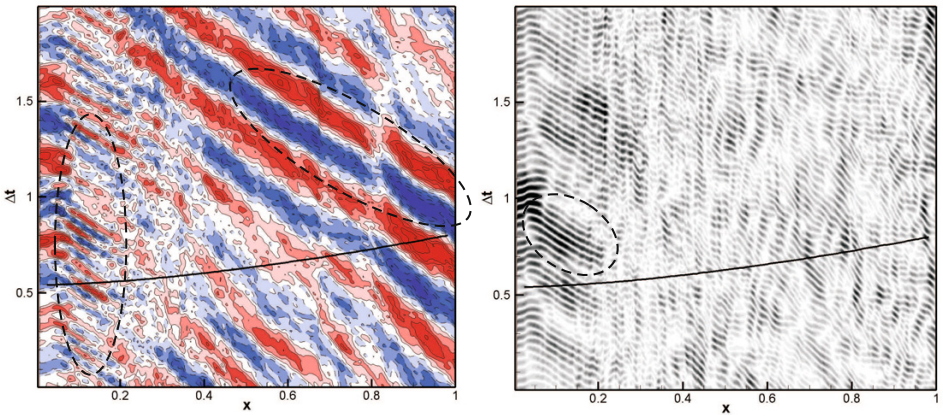

Figure 1: Cross correlation of surface pressure with pressure recorded at $(x, y) = (0.5, 1.5)$ for the flow around a NACA-0006 airfoil at $\alpha = 7°$, $Re = 5 \times 10^4$ and $M = 0.4$ for frequencies $f > 2$, with levels over the range $C_{pp} = \pm 0.25$ (left). Cross-correlation for frequency range $9 < f < 20$, showing absolute values over the range $0.03 < C_{pp} < 0.3$ (right). The black lines represent the mean acoustic propagation time and dashed lines highlight regions discussed in the text.

the desired frequency range to zero, and then reconstructing a time-series by computing the reverse Fourier transform.

The cross-correlation between surface pressure and pressure recorded above the airfoil at $(x, y) = (0.5, 1.5)$ for the flow around a NACA-0006 airfoil at $Re = 5 \times 10^4$, $\alpha = 7°$ and $M = 0.4$ is plotted in figure 1 (left). The variety of physical phenomena present result in a complex cross correlation compared to those obtained from, for example, turbulent jet flow [21], and correlation levels are comparatively higher. The strongest correlation is associated with downward sloping regions in the vicinity of the airfoil trailing-edge, and the mean acoustic-propagation time-line intersects a region of negative correlation at the airfoil trailing-edge. This feature is associated with the trailing-edge noise production mechanism, whereby the free-stream pressure correlates to downstream convecting fluctuations within the turbulent boundary layer, which ultimately generate acoustic waves as they convect over the airfoil trailing-edge. This behaviour is observed to be independent of observer location or flow conditions. In this case the upstream history of the noise production mechanism can be traced back to the transition location ($x = 0.2$), and the temporal wavelength of the correlation map near the trailing-edge indicates that low frequencies correlate more strongly here. In the region $0.075 < x < 0.2$ the correlation exhibits a spatio-temporal periodic pattern with decreased wavelength. In this region hydrodynamic instability waves are the largest amplitude pressure fluctuations present, and appear responsible for this feature of the correlation map. The fact that these instability waves are so clearly identifiable suggests one of two behaviours. The first possibility is that the transitional nature of the flow means that the frequency content of the flow is sufficiently narrowband that correlation levels are high for all frequencies (i.e. 'everything correlates to everything else'). It is also conceivable however that, analogous to the behaviour associated with trailing-edge noise, the upstream history of noise production due to transition is being elucidated.

Cross correlations are plotted for the frequency range $9 < f < 20$ in figure 1 (right). For this frequency interval the additional noise sources are expected to be the dominant source of airfoil self-noise. A first observation is that the trailing-edge region no longer exhibits a pronounced region of maximum correlation, hence confirming that the trailing-edge is not the dominant noise source in this frequency range. Instead, the most prominent region of maxima occurs in the range $0.05 < x <= 0.2$, displaced from the propagation time line by $\Delta t \approx 0.25$, and appears associated with hydrodynamic instability waves. If we assume that we are correlating to the upstream history of a hydrodynamic event that radiates noise (analogous to the trailing-

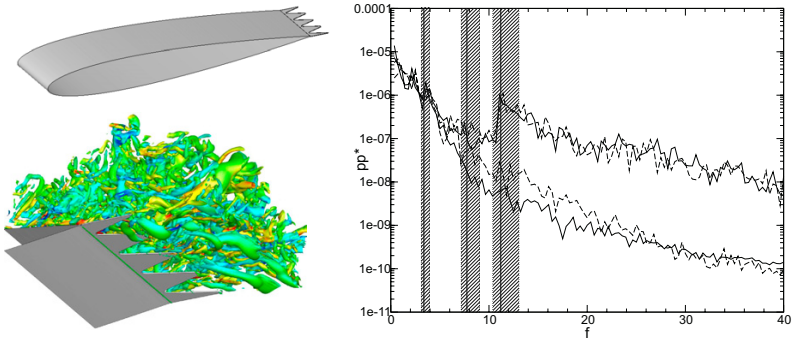

Figure 2: Airfoil geometry with serrated flat-plate TE extension (top left), iso-surfaces of $Q = 500$, coloured by streamwise vorticity for levels $[-100 : 100]$ for DNS of serrated TE (bottom left). Power pressure spectra taken above and below the airfoil at $(x, y) = (0.5, \pm 0.5)$ for airfoils with straight (- - -) and serrated (—) trailing-edges (right); vertical lines denote target frequencies and shaded areas show the range of frequencies used for one-third octave averages about the target frequencies.

edge mechanism discussed in the previous paragraph), we can trace downstream at the local convection velocity to the propagation time-line to yield an estimate for the noise source location at $x \approx 0.33$. This lies between the time-averaged transition and reattachment locations ($x = 0.2$ and $x = 0.39$ respectively). It is perhaps surprising, although consistent with previous studies [20], that the location of the additional sources cannot be isolated to a single location. It is hypothesised that the majority of the additional noise is produced at the reattachment point, where large amplitude pressure fluctuations are present in conjunction with stagnation-point flow into the airfoil surface. The inability to correlate to a clear-cut single location is attributed to the fact that the reattachment region is highly unsteady, the concept of a reattachment 'point' being valid only for the mean flow [18]. The location of noise production will therefore vary in the streamwise and spanwise directions, unlike the noise production mechanism at the airfoil trailing-edge which is fixed in space.

5. Trailing-edge serrations

For the investigation of the effect of trailing-edge serrations on the flow and acoustic fields NACA-0012 airfoils with serrated and straight flat plate extensions at the trailing-edge were selected. The advantage of a thin flat plate geometry is that bluntness effects are minimized. The flow conditions were chosen as $Re = 5 \times 10^4$, $M = 0.4$, and the incidence was set to $\alpha = 5°$ because previous simulations under these conditions exhibited a slightly thinner turbulent boundary layer, and greater tendency toward tonal behavior at low frequencies [11, 18]. A thinner boundary layer means that the trailing-edge serrations do not have to be unduly large and the presence of tonal noise at low frequency allows for investigation of the effect of serrations on tonal noise components. The serration geometry is described in more detail in Jones and Sandberg [19] and a schematic of the geometry is shown in figure 2 (left). The immersed boundary method is used only to represent the flat plate extensions to the airfoil trailing edge while a curvilinear C-type grid is body-fitted to the main body of the airfoil. A qualitative view of the flow in the vicinity of the trailing edge serrations is shown in figure 2 (left).

5.1. Effect on acoustic field

In Jones and Sandberg [19] instantaneous contours of dilatation rate indicated that the presence of trailing-edge serrations reduced the trailing-edge noise. The simulations have since been continued and are now statistically converged, allowing for analysis in the frequency domain. Power spectra of pressure from data of probe locations above and below the airfoil are shown in figure 2 (right) for the straight and serrated

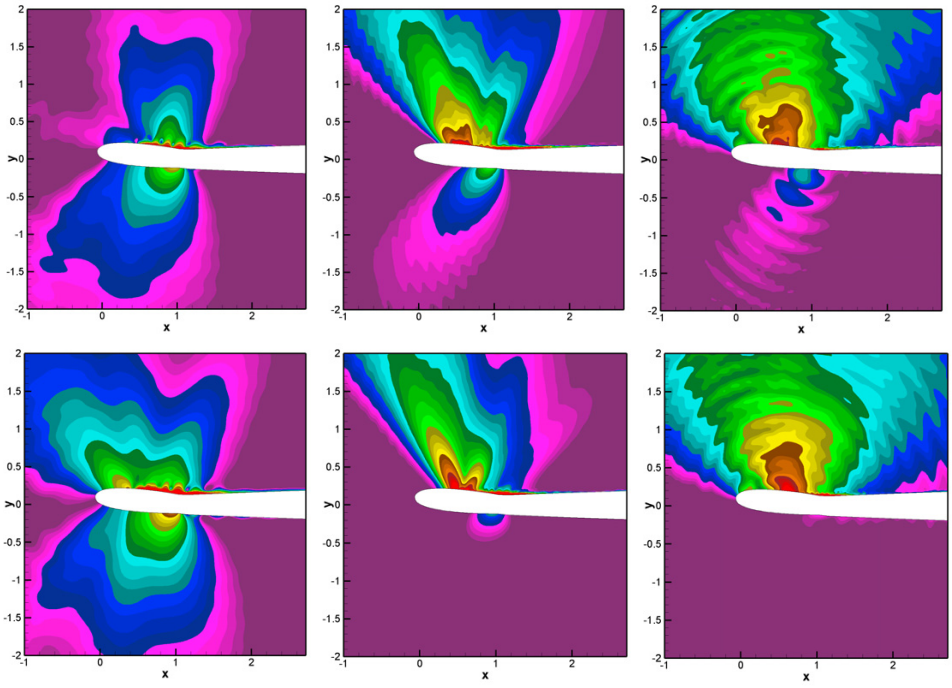

Figure 3: Logarithmically spaced contours of one-third octave averaged modulus of pressure for straight (top) and serrated (bottom) trailing edge; from left to right target frequency is $f = 3.37$, 7.75, 11.2.

trailing edge cases. Above the airfoil, where acoustic waves generated both at the airfoil trailing-edge and in the vicinity of transition are expected, the spectra appear in general to be similar in amplitude. Below the airfoil, where only trailing-edge noise is expected, for frequencies $f > 6$ the serrated trailing-edge simulation exhibits reduced amplitude pressure fluctuations compared to the straight trailing-edge simulation. Contrary to Howe's [9] analysis, the noise reduction does not occur for all frequencies above the threshold frequency, an effect also observed in experiments by Oerlemans *et al.* [10].

To visualize how the radiated sound field is modified by trailing-edge serrations, contours of modulus of pressure are shown in figure 3. Three target frequencies were chosen, shown in figure 2 (right) as vertical lines. One-third octave averaging about the target frequencies was performed to account for the broadband nature of the airfoil-noise. The lowest target frequency $f = 3.37$ is presumably mainly due to TE noise because the spectra obtained above and below the airfoil are similar. The mid-range frequency $f = 7.75$ corresponds to the most amplified frequency of instabilities in the laminar-turbulent transition region, and the highest frequency considered, $f = 11.2$, appears to be dominated by additional noise sources on the suction side considering the higher amplitudes of the pressure spectra obtained from above the airfoil.

According to Howe [9], no TE noise reduction can be expected from serrations with the current dimensions at the lowest frequency chosen. This is confirmed in figure 3 (left), where, considering the contours below the airfoil, no significant difference can be observed between the straight and serrated TE cases. The contrary is true for the higher frequencies shown. At $f = 7.75$ and $f = 11.2$ the trailing edge noise contribution appears considerably weakened by the addition of TE serrations. However, the addition of trailing edge serrations also appears to considerably change the noise radiation on the suction side of the airfoil at the lowest frequency, adding an upstream pointing lobe not present in the straight trailing edge case. This

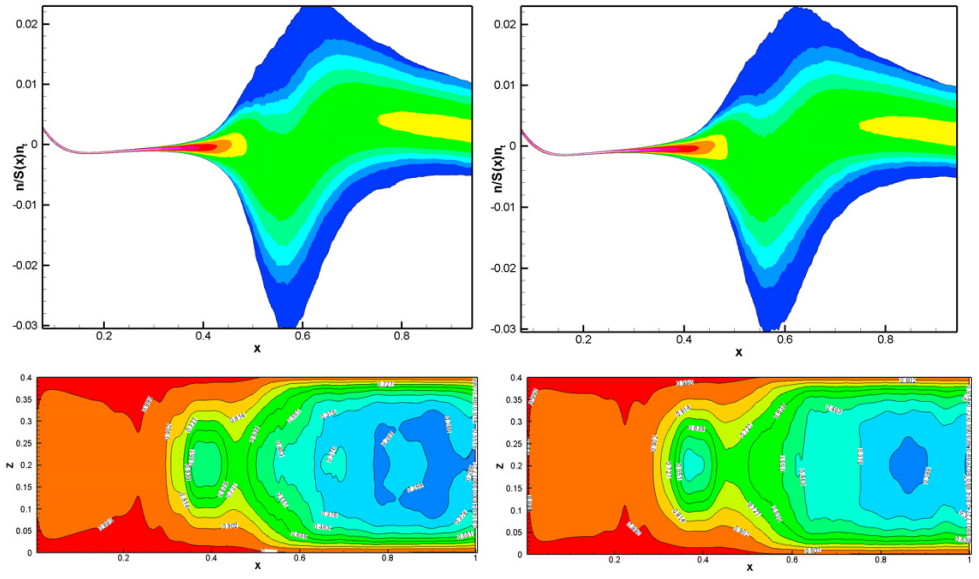

Figure 4: Contours of normalized probability density function of c_f (top) and contours of spanwise correlation function of pressure (bottom) for straight trailing edge (left) and serrated trailing edge (right).

was unexpected, especially in light of the fact that statistical quantities of turbulence and surface pressure spectra on the suction side of the airfoil were shown in Jones and Sandberg [19] to be highly similar for both cases. The effect of the TE serrations on the hydrodynamic field is therefore investigated again.

5.2. Effect on hydrodynamic field

An airfoil without trailing edge extension at the same flow parameters as chosen here was shown in Jones *et. al* [11] to be subject to an acoustic feedback loop in which sound waves generated at the trailing edge excite the boundary layer upstream of separation. Thus the question arises whether TE serrations might possibly affect the laminar-turbulent transition process in case the sound waves scattered off the trailing edge display a non-zero spanwise wavenumber which is then forced upon the laminar separation bubble and potentially alter the convective instability mechanism. Indeed, shed vortices upstream of transition visualized by iso-surfaces of Q display a spanwise variation for the serrated case [19]. The behaviour of the separation bubble is studied using probability density functions (PDF's) to account for its unsteadiness. Normalized PDF's of the skinfriction coefficient c_f on the suction surface of the airfoils are computed as described in Jones *et. al* [18]. Iso-contours of c_f PDFs over the upper airfoil surface are plotted in figure 4 (top) for straight and serrated trailing edges. The upper and lower PDF boundaries represent c_f at three standard-deviations from the mean, hence where the PDF is very narrow c_f varies only little with time, whereas where the PDF is wide c_f varies strongly. The main observation that can be made is that the two cases, surprisingly, are almost identical. This implies that the variation of the separation bubble length is similar, although the PDF's do not reveal any information on whether the oscillation about the mean occurs at the same frequencies. Figure 4 (bottom) shows the spanwise correlation function of pressure for the serrated and straight TE cases. It is difficult to identify any clear differences between the two cases. While the spanwise correlation is slightly decreased in the laminar-turbulent transition region, $x \approx 0.375$, the correlation is slightly increased at the aft end of the airfoil for the serrated case. Overall, it can also be concluded from the current results that the presence of serrations does not significantly affect

the hydrodynamic field, including the behaviour of the laminar separation bubble. Two reasons for why the hydrodynamic field is not considerably affected by the presence of serrations are suggested. Firstly, the feedback loop occurs at a frequency below the threshold frequency for which serrations are effective. Secondly, the three-dimensional instability mechanism reported in Jones *et al.* [18] dominates the transition process, thus even if the convective instability was forced differently it would not alter the transition process.

6. Conclusion

Direct numerical simulations of the flow around NACA-0006 and NACA-0012 airfoils at incidence were conducted with the aim of investigating transitional airfoil self-noise and the potential noise reduction of trailing-edge serrations. Cross-correlations of acoustic pressure in the farfield with pressure on the airfoil surface, combined with ray acoustic theory, clearly identify the trailing-edge noise mechanism by regions of large amplitude correlation located at the trailing-edge, at a retarded time associated with acoustic propagation from the source to observer location. It is suggested that the majority of the additional noise radiated on the suction side of the airfoil originates from the reattachment region rather than from the laminar-turbulent transition region. The additional noise, however, cannot be correlated cleanly to a single location on the airfoil as is the case for TE noise. This is most likely due to the fact that the reattachment region is highly unsteady and that the source locations therefore vary in space.

Power spectra of pressure recorded above and below the airfoil and one-third octave averaged contours of pressure show that trailing edge noise is reduced at higher frequencies while no significant difference is observed for TE noise at low frequencies and for noise generated in the reattachment region. The negligible effect of the trailing edge serrations on the hydrodynamic field is suggested to be due to either the fact that the feedback loop occurs at a frequency below the threshold frequency for which serrations are effective, and/or because the laminar-turbulent transition is dominated by a three-dimensional instability mechanism [18] which is unaffected by the serrations. In light of the hydrodynamic field being largely unaffected by the presence of trailing edge serrations, it is suggested that the trailing-edge noise reduction is mainly due to the effect of the serrations upon the diffraction process. Currently, the differences between the two geometries in low frequency noise radiation above the airfoil is still unaccounted for.

Acknowledgments

This work was supported by EPSRC grant EP/F048017/1. Part of the computer time was provided by the EPSRC grant GR/S27474/01.

[1] T. Brooks, D. Pope, M. Marcolini, Airfoil self-noise and prediction, NASA Reference Publication 1218, NASA (1989).
[2] J. Ffowcs Williams, L. Hall, Aerodynamic sound generation by turbulent flow in the vicinity of a scattering half plane, J. Fluid Mech. 40 (4) (1970) 657–670.
[3] M. J. Lighthill, On sound generated aerodynamically I. General theory, Proceedings of the Royal Society of London, Series A: Mathematical and Physical Science 211A (1107) (1952) 564–587.
[4] R. Amiet, Noise due to turbulent flow past a trailing edge, J. Sound and Vibration 47 (3) (1976) 387–393.
[5] C. K. W. Tam, H. Ju, Numerical simulation of the generation of airfoil tones at a moderate Reynolds number, AIAA Paper 2006–250212th AIAA/CEAS Aeroacoustics Conference (27th AIAA Aeroacoustics Conference), Cambridge, Massachusettes.
[6] R. D. Sandberg, L. E. Jones, N. D. Sandham, P. F. Joseph, Direct numerical simulations of tonal noise generated by laminar flow past airfoils, J. Sound and Vibration 320 (4–5) (2009) 838–858, doi:10.1016/j.jsv.2008.09.003.
[7] R. D. Sandberg, L. E. Jones, N. Sandham, Direct numerical simulations of noise generated by turbulent flow over airfoils, AIAA Paper 2008–286114th AIAA/CEAS Aeroacoustics Conference (29th AIAA Aeroacoustics Conference), Vancouver, Canada.
[8] M. Herr, W. Dobrzynski, Experimental investigations in low-noise trailing-edge design, AIAA journal 43 (6) (2005) 1167–1175.
[9] M. S. Howe, Noise produced by a sawtooth trailing edge, The Journal of the Acoustical Society of America 90 (1991) 482.
[10] S. Oerlemans, M. Fisher, T. Maeder, , K. Kogler, Reduction of Wind Turbine Noise using Optimized Airfoils and Trailing-Edge Serrations, AIAA Paper 08-2819, 14th AIAA/CEAS Aeroacoustics Conference, Vancouver, May.
[11] L. E. Jones, R. Sandberg, N. Sandham, An acoustic feedback instability of flow over an airfoil with a laminar separation bubble, Accepted for publication in J. of Fluid Mechanics.
[12] F. M. White, Viscous Fluid Flow, McGraw Hill, 1991.

[13] N. Sandham, Q. Li, H. Yee, Entropy splitting for high-order numerical simulation of compressible turbulence, J. Comp. Phys. 178 (2002) 307–322.
[14] R. D. Sandberg, N. D. Sandham, Direct numerical simulation of turbulent flow past a trailing edge and the associated noise generation, J. Fluid Mech. 596 (2008) 353–385.
[15] M. H. Carpenter, J. Nordström, D. Gottlieb, A stable and conservative interface treatment of arbitrary spatial accuracy, J. Comp. Phys. 148 (2) (1999) 341–365.
[16] H. Sandhu, N. D. Sandham, Boundary conditions for spatially growing compressible shear layers, Report QMW-EP-1100, Faculty of Engineering, Queen Mary and Westfield College, University of London.
[17] R. D. Sandberg, N. D. Sandham, Nonreflecting zonal characteristic boundary condition for direct numerical simulation of aerodynamic sound, AIAA J. 44 (2) (2006) 402–405.
[18] L. E. Jones, R. Sandberg, N. Sandham, Direct numerical simulations of forced and unforced separation bubbles on an airfoil at incidence, J. Fluid Mech. 602 (2008) 175–207.
[19] L. E. Jones, R. D. Sandberg, Direct numerical simulations of noise generated by the flow over an airfoil with trailing edge serrations, AIAA Paper 2009–319515th AIAA/CEAS Aeroacoustics Conference (30th AIAA Aeroacoustics Conference), Miami, Florida.
[20] L. E. Jones, R. D. Sandberg, N. Sandham, Investigation and prediction of transitional airfoil self-noise, AIAA Paper 2009–3104, 15th AIAA/CEAS Aeroacoustics Conference (30th AIAA Aeroacoustics Conference), Miami, Florida.
[21] C. Bogey, C. Bailly, An analysis of the correlations between the turbulent flow and the sound pressure fields of subsonic jets, Journal of Fluid Mechanics 583 (2007) 71–97.